

Double-resonance spectroscopy in Rubidium vapour-cells for high performance and miniature atomic clocks

M Gharavipour¹, C Affolderbach¹, S Kang², and G Mileti¹

¹Laboratoire Temps-Fréquence, Institut de Physique, Université de Neuchâtel, Switzerland

²Time and Frequency Division, National Institute of Standards and Technology, Boulder, Colorado, USA

Email: gaetano.mileti@unine.ch

Abstract. We report our studies on using microwave-optical double-resonance (DR) spectroscopy for a high-performance Rb vapour-cell atomic clock in view of future industrial applications. The clock physics package is very compact with a total volume of only 0.8 dm³. It contains a recently in-house developed magnetron-type cavity and a Rb vapour cell. A home-made frequency-stabilized laser system with an integrated acousto-optical-modulator (AOM) – for switching and controlling the light output power– is used as an optical source in a laser head (LH). The LH has the overall volume of 2.5 dm³ including the laser diode, optical elements, AOM and electronics. In our Rb atomic clock two schemes of continuous-wave DR and Ramsey-DR schemes are used, where the latter one strongly reduces the light-shift effect by separation of the interaction of light and microwave. Applications of the DR clock approach to more radically miniaturized atomic clocks are discussed.

1. Introduction

Microwave-optical double-resonance (DR) spectroscopy in alkali vapour cells constitutes simultaneously a field of basic research and of more application-oriented developments of precision instruments such as frequency standards and magnetometers [1]. In the case of atomic frequency standards (atomic clocks), the frequency of an oscillator, for example quartz, is stabilized to the atomic resonance by an electronic servo-loop (see figure 1).

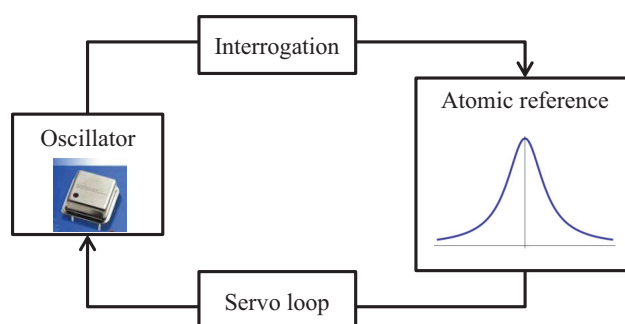


Figure 1. Basic principle in atomic clocks.

Historically, the first investigations were realized with alkali plasma discharge lamps as optical source while the radio-frequency (rf) or microwave field was applied using different techniques such as simple metallic loops, antennas, horns or resonant cavities. The various types of optical pumping processes [2] and the AC Stark shift induced on the rf or microwave atomic transitions by the resonant optical field were investigated in great details from both the experimental and the theoretical points of view [3, 4]. Different techniques inspired by the Nuclear Magnetic Resonance (NMR) methods were also developed in order to study the sources of relaxations (in particular the collisions) [5]. In the case of Rubidium atomic vapour cells, the presence of two isotopes with partially overlapping optical transitions allowed to improve the efficiency of the hyperfine optical pumping, thanks to the so-called “isotopic filtering”, and resulted in the realization of commercial atomic frequency standards that were required in many applications such as network synchronization, secure telecommunication and satellite positioning and navigation systems [6, 7, 8]. Recently portable standards such as the space passive hydrogen maser (SPHM) [9] or laser-beam CS beam clocks (LPCs) [10] show the short-term stability for one second averaging time $7 \times 10^{-13} - 1.5 \times 10^{-12}$ and the long-term stability for one day $1 \times 10^{-14} - 3 \times 10^{-14}$ with the volume range typically from 13 to 28 dm³. In compact cell-type clocks of interest here, the accuracy and the medium- to long-term frequency stability are ultimately limited by the fact that the atoms are stored in a thermal vapour cell with unavoidable collisions which effects are very sensitive to the environmental changes and other aging processes.

In this present investigation we report on our highly-compact Rb atomic clock based on microwave-optical DR interrogation in both continuous-wave (CW) mode [11] and pulsed [12] Ramsey-DR scheme [13, 14]. We show that with both CW-DR and Ramsey-DR schemes, the achieved short- and the long-term frequency stability of our Rb atomic clock are comparable with the ones from SPHM or cold atoms portable clocks [15].

2. Double-Resonance schemes

In a DR atomic clock two resonant electromagnetic fields of light and microwave are required for both CW-DR and Ramsey-DR schemes. The optical field by using a laser, in our case acting on Rb D2 line at 780 nm, prepares –with optical pumping– and probes –with optical detection– the atomic states of the reference –in our case Rb. The microwave field samples the so-called clock frequency which is the frequency of the clock transition of the atomic reference by using a microwave generator. In our ⁸⁷Rb atomic clock the clock transition is the $5^2S_{1/2} |F_g=1, m_F=0\rangle \leftrightarrow |F_g=2, m_F=0\rangle$ with the frequency of $\nu_{Rb} = 6\,834\,682\,610.900312$ Hz [16]. The three steps of optical pumping, microwave interrogation and optical detection are applied simultaneously in the case of CW-DR, while they are separated in time in the case of Ramsey-DR scheme (see figures 2(b) and 2(c)). This separation can suppress the light shifts (LS) effect in Ramsey-DR scheme, but it requires an additional component like an acousto-optical-modulator (AOM) as an optical switch. It makes this scheme slightly more complex and increases the volume and the power consumption compared to CW-DR scheme.

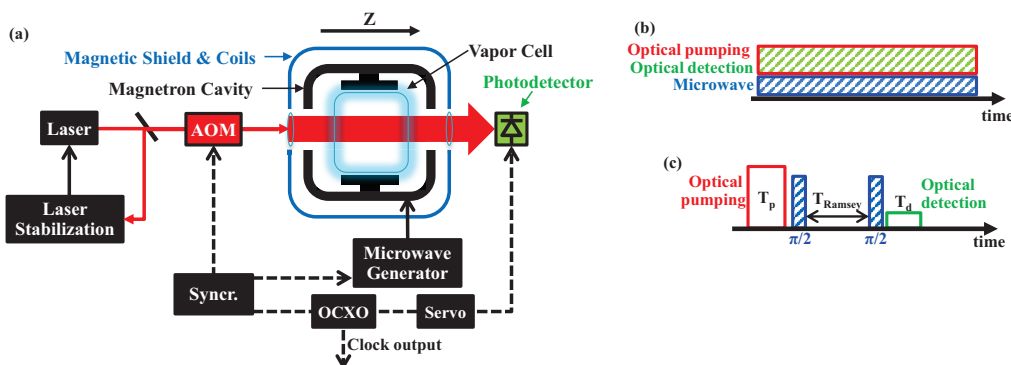


Figure 2. (a) Schematic setup for CW-DR and Ramsey-DR clocks. The AOM is used only in the case of Ramsey-DR scheme. (b) CW-DR sequences. (c) Ramsey-DR sequences.

3. High-performance Rb atomic clock

The atomic clock setup is shown schematically in figure 2(a). The main clock hardware components are: 1) the Laser source, 2) the Physics Package (PP) and 3) the local oscillator (LO). In the following, we briefly describe the laser source and the PP. The LO was described in details in [17].

3.1. The Laser source

A distributed-feedback (DFB) laser diode emitting at 780 nm (Rb D2 transition) is placed in a compact laser head (LH) used as the laser source. Moreover, an evacuated ^{87}Rb reference cell which is thermally controlled and an AOM are integrated in the LH assembly [18]. Figure 3 shows the schematics of the optical setup of the LH. The optical components in the LH occupy 1 dm^3 only while its overall volume is 2.4 dm^3 , including space for control electronics. The total power consumption for the laser supply and heaters (laser, reference cell and baseplate) is less than 1.5 W at ambient temperature. The frequency of the laser is stabilized to the sub-Doppler absorption lines using an evacuated ^{87}Rb reference cell. The AOM that is used for fine tuning of the laser frequency and also as a fast switch, with rise and fall times $< 5\ \mu\text{s}$ to control the durations and output powers of optical pumping and optical detection pulses. The laser has an emission linewidth of $< 2\text{ MHz}$ and shows a fractional frequency stability below 1×10^{-11} . All these characteristics make the LH appropriate for use in the DR atomic clock setup.

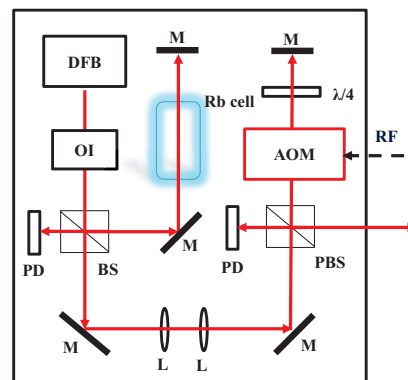


Figure 3. Schematics of the optical setup of the LH.

3.2. The Physics Package

The clock Physics Package (PP), with overall volume of 0.8 dm^3 , contains a vapour cell, the magnetron type cavity, a C-field coil, a magnetic shield and an optical detector. The vapour cell is made of glass and is developed in-house. It is filled with ^{87}Rb atomic vapour and a mixture of Argon and Nitrogen buffer-gases of 26 mbar total pressure with the ratio of $P_{\text{Ar}}/P_{\text{N}_2}=1.6$. The vapour cell has a cylindrical shape with a diameter of 25 mm and a height of 25 mm. The cell has a stem acting as a reservoir for the Rb atoms. It is placed in a compact so-called magnetron-type cavity based on a loop-gap resonator approach. The cavity has a total external volume of 45 cm^3 which resonates at the ^{87}Rb clock's transition frequency of $\approx 6.835\text{ GHz}$, in a TE_{011} -like mode with a relatively low loaded quality factor $Q \approx 200$ [19]. The cavity is mounted inside a C-field coil that creates a static magnetic field parallel to the laser propagation vector (z direction) to split the respective Zeeman levels of ^{87}Rb hyperfine ground states. The field orientation factor (FOF), ξ , –which describes the fraction of useful magnetic field driving the clock transition with respect to the total field energy over the entire cell volume– can characterize the uniformity of the microwave magnetic field distribution inside the cavity [19]. In our magnetron-type cavity ξ was measured up to 0.95% that guarantees a strong clock signal. Moreover, the achieved high-contrast Ramsey signal and Rabi oscillations prove the homogeneity of the microwave magnetic field distribution [14]. A two-layer magnetic shield surrounds the whole PP to shield against external magnetic field fluctuations. A photodetector collects the transmitted light behind the cell.

3.3. Clock signals and short-term stability

The recorded clock signals for both CW-DR and Ramsey-DR schemes applied to the same Rb atomic clock setup are shown in figure 4. For CW-DR mode (the solid red line in figure 4), the signal has a contrast of $C=26\%$ and its linewidth of $\Delta\nu_{1/2}=334$ Hz is limited by optical and microwave power broadening here [11]. In the case of Ramsey-DR scheme (the dashed blue line in figure 4) the central fringe has a contrast of $C=40\%$ and a linewidth of $\Delta\nu_{1/2}=160$ Hz, limited by the 3 ms Ramsey time, T_{Ramsey} (duration between two $\pi/2$ microwave pulses, see figure 2(c)).

The measured short-term stability of the clock is limited by the shot-noise [11], the signal to noise ratio [20] and the microwave noise from the LO through the Dick effect [21]. This short-term stability is measured on the levels of $1.4 \times 10^{-13} \tau^{-1/2}$ and $2.4 \times 10^{-13} \tau^{-1/2}$ for CW-DR and Ramsey-DR schemes, respectively [22]. In the case of CW-DR scheme, the shot-noise limit contribution is at the level of $4.9 \times 10^{-14} \tau^{-1/2}$. It is about three times higher than the one from Ramsey-DR ($1.7 \times 10^{-14} \tau^{-1/2}$ [22]) which is explained by the lower light intensity during the optical detection in the Ramsey scheme. In both CW-DR and Ramsey schemes, the dominant instability contribution in the short-term stability is due to technical laser noise and FM-to-AM noise conversion in the vapour cell [14, 19]. In the case of Ramsey-DR, additional noise from the AOM [14] results in slight degradation of the short-term stability of the clock compared to CW-DR case.

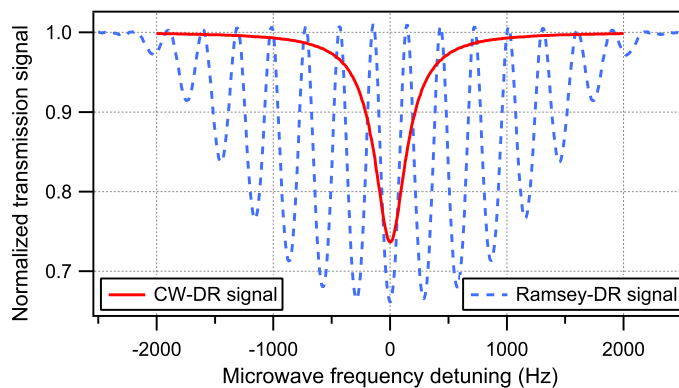


Figure 4. Double resonance signal in the case of the CW-DR scheme (solid red line) compared to Ramsey fringes in the case of Ramsey-DR (dashed blue line) [11, 14].

3.4. Limitations to long-term stability

Generally, in DR vapour-cell atomic clocks the long-term stability at $\tau = 10^4$ s to one day is limited by systematic variations of various parameters like the cell temperature and the input powers and frequencies of the light and microwave that can perturb the clock frequency. On the long-term clock stability of our Rb atomic clock, the contributions from the temperature shift and the light shifts (LS) are the dominating contributors, for both CW-DR and Ramsey-DR schemes [23]. The geometry of the vapour cell affects the temperature shift [24]: for example, the temperature coefficient (TC) improved by an order of magnitude for a newly-designed vapour cell with a shorter stem to 5.5×10^{-15} . The LS intensity and frequency coefficients α and β , respectively, were measured in the same Rb clock setup where the laser frequency was stabilized to the sub-Doppler cross-over transition CO11-12 for both CW-DR and Ramsey-DR schemes. The results are shown in table 1. It can be seen that α and β are suppressed about 5 and 125 times, respectively, from CW-DR to Ramsey-DR scheme as a consequence of the separation of the light and microwave interaction in the case of Ramsey-DR. The LS can be completely suppressed in Ramsey-DR, potentially, if no light passes through the cell unless during the optical pumping and the optical detection pulses. In our setup, the fraction of the residual light intensity to the optical pumping intensity was measured about 0.0005 which thus gives rise to the residual LS measured.

Table 1. LS intensity and frequency coefficients for both CW-DR and Ramsey-DR Rb clocks.

	CW-DR	Ramsey-DR
LS intensity coeff. α (/%)	3.5×10^{-13}	-6.6×10^{-14}
LS frequency coeff. β (/MHz)	-1.0×10^{-11}	-8.0×10^{-14}

4. Miniature clock

In parallel to the studies on high-performance atomic clocks described in section 3, we have conducted several studies towards further miniaturization of atomic clocks, notably in view of mobile applications and low power-consumption devices [25]. One focus of these studies concerns microwave-optical double resonance in micro-fabricated vapour cells [26], which constitutes a very promising alternative to the Coherent Population Trapping (CPT) approach widely pursued for chip-scale atomic clocks [27]. In fact, for an atomic vapour cell of same size the DR scheme allows reaching higher clock signal amplitude and thus better clock stability than the (CPT) scheme. With our collaboration partners we have developed several different designs and geometries of micro-fabricated alkali vapour cells, including e.g. a 4mm-size Rb vapour cell based on multi-stack anodic bonding of silicon and glass wafers [28] (Figure 5). Combined with a miniaturized microwave resonator cavity, the micro-loop-gap resonator [29], clock stabilities on the level of $7 \times 10^{-12} \tau^{-1/2}$ were obtained, which are of high interest for future miniature atomic clocks, for example in view of smart-grid applications. We also demonstrated double-resonance spectroscopy in a miniature vapour cell using a micro-fabricated discharge lamp as light source [30], as an alternative to laser-based chip-scale atomic clocks.

A potential alternative to existing approaches consists in covering the inner walls of the alkali vapour cell with an “anti-relaxation” coating [31]. This approach is particularly interesting in micro-fabricated vapour cells, where the high buffer-gas pressures required generally result in a loss of signal amplitude. However, the use of anti-relaxation wall coatings in micro-fabricated cells has been long time hindered by the incompatibility of temperature ranges for operational wall coatings and established cell-sealing techniques. After an initial study on the metrological properties of an atomic clock based on a cm-scale glass-blown wall-coated cell [32], we could demonstrate a first micro-fabricated vapour cell with an operational anti-relaxation wall-coating, based on a dedicated low-temperature sealing technique [33].

The pulsed Ramsey-DR clock scheme with its advantage of reduced light-shift demonstrated for the much bigger high-performance atomic clocks could also be applied to the realm of miniature atomic clocks. Our numerical simulations show that this approach should allow observation of high-quality Ramsey fringes from a micro-fabricated vapour cell, compatible with a clock stability on the level of $\leq 10^{-11} \tau^{-1/2}$ [22]. Combined with recently demonstrated pulsed laser interrogation for miniature atomic clocks using laser current modulation only [34], this approach bears high promise for the realization of strongly miniaturized atomic clocks with reduced light-shift effect and thus improved long-term stability.



Figure 5. Micro-fabricated Rb vapour cell with 4mm-thick core and excellent control of the cell geometry, manufactured by multi-stack anodic bonding [28]. The photo shows the cell on top of a 1 euro-cent coin.

5. Conclusion

We have studied high-performance Rb vapour cell atomic clocks based on microwave-optical DR using a very small magnetron-type microwave cavity in view of highly compact clock device. The clock was operational in both CW-DR and Ramsey-DR schemes. An integrated AOM in the frequency-stabilized laser system allowed us to separate optical and microwave pulses Ramsey-DR scheme. In both schemes, the optical detection noise was the main limitation in short-term clock stability while on the long-term scales ($\tau \approx 10^4$ s) the temperature sensitivity from the vapour cell and light-shift effects dominated. The vapour cell TC can be controlled by the geometry and design of the cell and the LS can be suppressed by switching from CW-DR to Ramsey-DR scheme. Based on previous developments, application of the Ramsey interrogation scheme also to strongly miniaturized Rb DR clocks appears possible.

Acknowledgments

This work was supported by the Swiss National Science Foundation (SNSF grant no. 140712) and the European Metrology Research Programme (EMRP project IND55-Mclocks). The EMRP is jointly funded by the EMRP participating countries within EURAMET and the European Union. We also acknowledge previous support from the European Space Agency (ESA) and the Swiss Space Office (Swiss Confederation). We thank A. K. Skrivervik, C. Stefanucci, and A. E. Ivanov (all EPFL-LEMA) for their support on the microwave cavity, and C. Calosso (INRIM, Italy) for the microwave LO. We thank T. Bandi and M. Pellaton for their contributions to the early phases of the work, and our co-authors of our cited references for fruitful collaborations.

References

- [1] Camparo J 2007 *Phys. Today*, **60** 33
- [2] Kastler A 1950 *J. Phys. Radium*, **11** 255
- [3] Cohen-Tannoudji C and Barrat J 1961 *J. Phys. Radium*, **22** 329
- [4] Mathur B S, Tang H and Happer H 1968 *Phys. Rev.*, **171** 11
- [5] Franzen W 1959 *Phys. Rev.*, **115** 850
- [6] Dupuis R T, Lynch T J and Vaccaro J R 2008 *Proc. IEEE Int. Frequency Control Symposium* edited by Jadusliwer B. (*Honolulu, Hawaii, USA 19-21 May 2008*) pp. 655-660
- [7] Waller P, Gonzalez S, Binda S, Sesia I, Hidalgo I, Tobias G and Tavella P 2010 *IEEE Trans. Ultrason. Ferroelect. Freq. Cont.*, **57** 738
- [8] Chunhao H, Zhiwu C, Yuting L, Li L, Shenghong X, Lingfeng Z and Xianglei W 2013, *Int. J. Navig. Observ.* **2013** 371450
- [9] Rochat P, *et al.* 2005 *Proc. IEEE Frequency Control Symp., Vancouver, BC, USA*, pp. 26–32
- [10] Lecomte S, *et al.* 2007 *Proc. IEEE Frequency Control Symp. and 21st European Frequency and Time Forum, Geneva, Switzerland*, pp. 1127 – 1131
- [11] Bandi T, Affolderbach C, Stefanucci C, Merli F, Skrivervik A K and Mileti G 2014 *IEEE Trans. Ultrason. Ferroelect. Freq. Cont.*, **61** 1769-1778
- [12] Micalizio S, Godone A, Levi F and Calosso C 2009 *Phys. Rev. A.*, **79** 013403
- [13] Kang S, Affolderbach C, Gruet F, Gharavipour M, Calosso C E and Mileti G 2014 *Proc. 26th European Frequency and Time Forum (EFTF) (Neuchatel, Switzerland, 23-26 June 2014)* pp. 544-547
- [14] Kang S, Gharavipour M, Affolderbach C, Gruet F and Mileti G 2015 *J. Appl. Phys.*, **117** 104510
- [15] Esnault F X, Rossetto N, Holleville D, Delporte J and Dimarcq N 2011 *J. Adv. Space Res.*, **47** (5) pp. 854–858
- [16] Guéna J, Abgrall M, Clairon A and Bize S 2014, *Metrologia*, **51** 108–120
- [17] Calosso C E, Micalizio S, Godone A, Bertacco E K and Levi F 2007 *IEEE Trans. Ultrason., Ferroelect. Freq. Control.* **54** 1731
- [18] Gruet F, Pellaton M, Affolderbach C, Bandi T, Matthey R and Mileti G 2012 *Proc. Int. Conf. on Space Optics (ICSO) (Ajaccio, Corsica, 9-12 October 2012)* no. 48

- [19] Stefanucci C, Bandi T, Merli F, Pellaton M, Affolderbach C, Mileti G and Skrivervik A K 2012 *Rev. Sci. Instrum.*, **83** 104706
- [20] Micalizio S, Calosso C E, Godone A and Levi F 2012 *Metrologia*, **49** 425-436
- [21] Deng J Q, Mileti G, Drullinger R E, Jennings D A, and Walls F L 1999 *Phys. Rev. A*, **59** 773
- [22] Gharavipour M, Affolderbach C, Kang S, Bandi T, Gruet F, Pellaton M and Mileti G 2016 *Jour. of Phys.: Conference Series* **723** 012006
- [23] Affolderbach C, Gharavipour M, Kang S, Gruet F and Mileti G 2015 *Proc. 5th International Colloquium on Scientific and Fundamental Aspects of the Galileo Programme, Braunschweig, Germany, October 27-29, 2015*
- [24] Calosso C E, Godone A, Levi F and Micalizio S 2012, *IEEE Trans. Ultrason., Ferroelect. Freq. Control.* **59** No. 12
- [25] Knappe S 2007 *Comprehensive Microsystems* vol 3, ed. Gianchandani Y, Tabata O and Zappe H (Amsterdam: Elsevier) p 571
- [26] Pellaton M, Affolderbach C, Petremand Y, de Rooij N F and Mileti G 2012 *Physica Scripta* **T149** 014013
- [27] Lutwak R, Emmons D, Riley W and Garvey R M 2002 *Proc. 34th Annual Precise Time and Time Interval (PTTI) Meeting* (Reston, VA, 3–5 Dec. 2002) pp 539–550
- [28] Pétremand Y, Affolderbach C, Straessle R, Pellaton M, Briand D, Mileti G and de Rooij N F 2012 *Journal of Micromechanics and Microengineering* **22** 025013
- [29] Violetti M, Pellaton M, Merli F, Zürcher J–F, Affolderbach C, Mileti G and Skrivervik A K *IEEE Journal of Sensors* **14** 9
- [30] Venkatraman V, Kang S, Affolderbach C, Shea H and Mileti G 2014 *Appl. Phys. Lett.*, **104** 054104
- [31] Robinson H G and Johnson C E 1982 *Appl. Phys. Lett.*, **40** 771
- [32] Bandi T, Affolderbach C and Mileti G 2012 *J. Appl. Phys.*, **111** 124906
- [33] Straessle R, Pellaton M, Affolderbach C, Pétremand Y, Briand D, Mileti G and de Rooij N F 2014 *Appl. Phys. Lett.* **105** 043502
- [34] Ide T, Goka S and Yano Y 2015 *Proc. Joint Conf. IEEE Int. Frequency Control Symposium & European Frequency and Time Forum (EFTF) (Denver, Colorado, USA 12-16 April 2015)*, pp. p 167